Title
Resonant neutrino spin-flavor precession and supernova nucleosynthesis and dynamics

Permalink
https://escholarship.org/uc/item/7s47x230

Journal
Physical Review D, 55(6)

ISSN
2470-0010

Authors
Nunokawa, H
Qian, Y-Z
Fuller, GM

Publication Date
1997-03-15

DOI
10.1103/physrevd.55.3265

Peer reviewed

Resonant neutrino spin-flavor precession and supernova nucleosynthesis and dynamics

H. Nunokawa,* Y.-Z. Qian,† and G. M. Fuller‡

Institute for Nuclear Theory, University of Washington, Box 351550, Seattle, Washington 98195

(Received 10 October 1996)

We discuss the effects of resonant spin-flavor precession (RSFP) of Majorana neutrinos on heavy element nucleosynthesis in neutrino-heated supernova ejecta and the dynamics of supernovae. In assessing the effects of RSFP, we explicitly include matter-enhanced (MSW) resonant neutrino flavor conversion effects where appropriate. We point out that for plausible ranges of neutrino magnetic moments and protoneutron star magnetic fields, spin-flavor conversion of ν_τ (or ν_μ) with a cosmologically significant mass (1–100 eV) into a light $\bar{\nu}_e$ could lead to an enhanced neutron excess in neutrino-heated supernova ejecta. This could be beneficial for models of r-process nucleosynthesis associated with late-time neutrino-heated ejecta from supernovae. Similar spin-flavor conversion of neutrinos at earlier epochs could lead to an increased shock reheating rate and, concomitantly, a larger supernova explosion energy. We show, however, that such increased neutrino heating likely will be accompanied by an enhanced neutron excess which could exacerbate the problem of the overproduction of the neutron number $N = 50$ nuclei in the supernova ejecta from this stage. In all of these scenarios, the average $\bar{\nu}_e$ energy will be increased over those predicted by supernova models with no neutrino mixings. This may allow the SN 1987A data to constrain RSFP-based schemes. [S0556-2821(97)04406-8]

PACS number(s): 97.60.Bw, 12.15.Ff, 14.60.Pq, 97.10.Cv

I. INTRODUCTION

In this paper we examine the effects of resonant spin-flavor precession (RSFP) of Majorana neutrinos on heavy element nucleosynthesis in neutrino-heated supernova ejecta and the dynamics of supernovae. Massive neutrinos that possess a transition magnetic moment could experience a resonant conversion of spin and flavor in the presence of magnetic fields and matter [1,2]. This RSFP effect is similar to the well-known Mikheyev-Smirnov-Wolfenstein (MSW) mechanism [3]. In fact, in the environment above the neutrinosphere in post-core-bounce supernovae, both the MSW and RSFP processes may operate. Reference [4] discusses the effect of RSFP-induced neutrino flavor conversion on supernova shock reheating. Here we extend their discussion by considering the effects of RSFP on nucleosynthesis in late-time neutrino-heated supernova ejecta and generally including the effects of *both* RSFP *and* MSW conversion.

Supernovae have long been considered as a promising site for heavy element nucleosynthesis [5]. About one-half of the elements with mass number $A > 70$ in nature are believed to be made by the rapid neutron capture process, or r process for short. In the r process, neutron captures occur much faster than typical β decays. Recent calculations suggest that the high-temperature, high-entropy region which would be formed above the protoneutron star several seconds after the bounce of the core in a type-II supernova is a promising site for r-process nucleosynthesis [6,7,8].

This site is sometimes referred to as the ''hot bubble,'' since material there is heated by absorption of neutrinos and antineutrinos which are emitted from the neutrinosphere near the surface of the hot protoneutron star. Close to the neutrinosphere the temperature is high enough that all strong and electromagnetic nuclear interactions are in equilibrium [nuclear statistical equilibrium (NSE)]. As the material above the neutrinosphere expands due to neutrino heating, its temperature and density decrease. When the temperature drops below about 0.5 MeV, the material outflow rate (or expansion rate) becomes faster than the rates for nuclear reactions. At this point, the material freezes out of NSE. As the material further expands above this nuclear freeze-out point, rapid neutron captures onto the existing seed nuclei may occur after an α-rich freeze-out of the charged-particle reactions.

In order for the r process to occur, the material certainly has to be neutron-rich at the nuclear freeze-out position. The neutron-to-proton ratio above the neutrinosphere is determined by the reactions

$$\nu_e + n \rightarrow p + e^-, \tag{1a}$$

$$\bar{\nu}_e + p \rightarrow n + e^+. \tag{1b}$$

Because material in the surface layers of the protoneutron star consists mostly of neutrons, ν_e have a larger opacity than $\bar{\nu}_e$ [see Eqs. (1a) and (1b)]. Consequently, $\bar{\nu}_e$ decouple deeper inside the protoneutron star where it is hotter, and correspondingly have a higher average energy than ν_e. In turn, this average energy hierarchy favors the rate of the process in Eq. (1b) over that in Eq. (1a). These arguments suggest that neutron-rich conditions which are conducive to

---

*Present address: Instituto de Física Corpuscular-CSIC, Departament de Física Teòrica, Universitat de València, 46100 Burjassot, València, Spain.

†Present address: Department of Physics, 161-33, California Institute of Technology, Pasadena, California 91125.

‡Permanent address: Department of Physics, University of California, San Diego, La Jolla, California 92093-0319.

r-process nucleosynthesis will obtain at the nuclear freeze-out point and beyond, in the region where the r process may occur.

Reference [9] discusses these weak reaction issues and the connection between the flavor mixing of neutrinos with cosmologically significant masses and the conditions necessary for heavy element nucleosynthesis in supernovae. It was shown in Ref. [9] that resonant flavor conversion of a ν_τ or ν_μ with a mass of 1–100 eV into a light ν_e may preclude heavy element nucleosynthesis in the hot bubble unless the vacuum mixing angle satisfies $\sin^2 2\theta \lesssim 10^{-5}$. Because ν_μ and ν_τ and their antineutrinos lack the charged-current reactions similar to those in Eqs. (1a) and (1b), they decouple deepest inside the protoneutron star and have the highest average energy. Consequently, a significant amount of $\nu_{\tau(\mu)} \leftrightarrow \nu_e$ transformation results in ν_e with an average energy higher than that of $\overline{\nu}_e$. This enhances the rate of the process in Eq. (1a) and drives the neutrino-heated supernova ejecta proton-rich.

If the mass of ν_τ (or ν_μ) is between about 1 and 100 eV, then matter-enhanced resonant MSW flavor conversion could occur in the region between the neutrinosphere and the radius where the weak reactions in Eqs. (1a) and (1b) freeze out (very near the nuclear freeze-out position in most supernova models). If average energy ν_μ or ν_τ are converted at resonance with greater than about (25–30)% efficiency, then the hot bubble will be driven proton-rich and r-process nucleosynthesis at this site will be impossible.

With no such flavor conversion, the neutron excess required for r-process nucleosynthesis may or may not be obtained currently in models of neutrino-heated supernova ejecta. Although the conditions of entropy, electron fraction [a measure of the neutron-to-proton ratio and the neutron excess, see Eq. (11)], and expansion rate as computed in some hydrodynamic models [8] provide the requisite neutron-to-seed ratio for the r process to occur, these models have left out key physics input that can wreck the r process [10]. Besides, simple wind model arguments suggest that the neutron-to-seed ratio obtained in these hydrodynamic models is unrealistically large on account of their high entropies at late times. Wind models suggest an entropy roughly half of that obtained in some hydrodynamic models, and this would imply a neutron-to-seed ratio too low to allow the production of the heaviest r-process nuclides [11,12].

Any effect that could *lower* the electron fraction Y_e (i.e., raise the neutron-to-seed ratio) in these models would be most welcome. In fact, it is even conceivable that r-process nucleosynthesis in late-time neutrino-heated supernova ejecta will be impossible unless there is some new physics which has the effect of raising the neutron excess [13,14]. However, any effect that significantly lowers Y_e at late times must not also do so at the early times characteristic of shock reheating, lest the neutron number $N=50$ nuclei be overproduced [8,15,16]. This shock reheating epoch occurs roughly ~ 0.1–0.6 s after core bounce, as opposed to the epoch where the r process might take place in neutrino-heated ejecta at ~ 3–20 s after core bounce.

In what follows we show that ν_τ (or ν_μ) with vacuum masses in the range 1–100 eV could convert in principle into $\overline{\nu}_e$ by RSFP above the neutrinosphere. In turn, this could lead to the *enhancement* of the neutron excess in the ''hot

bubble.'' In order to have the conversion $\nu_{\tau(\mu)} \leftrightarrow \overline{\nu}_e$, neutrinos must be of Majorana-type and have a finite transition magnetic moment. The operation of RSFP also requires a (probably large) magnetic field around the protoneutron star. If RSFP did occur, $\overline{\nu}_e$ would become much more energetic than ν_e and this would enlarge the neutron-to-proton ratio as outlined above. This implies that RSFP could be beneficial to the production of the heavier r-process elements in supernovae, in contrast to the case of resonant MSW flavor conversion alone as discussed in Ref. [9]. For significant RSFP effects to occur, the required product of the neutrino transition magnetic moment μ_ν and magnetic field B near the neutron star will be shown to be of order 1 in units of Bohr magneton times Gauss ($\mu_B\ G$).

Before entering into a detailed discussion of RSFP in supernovae, let us describe the present upper limits on the neutrino magnetic moment from laboratory experiments and astrophysical arguments. The present upper bound on the neutrino magnetic moment from $\overline{\nu}_e e$ scattering experiments is [17]

$$\mu_\nu < 1.9 \times 10^{-10} \mu_B. \tag{2}$$

This bound applies to the direct or transition magnetic moment of Dirac neutrinos, as well as the transition magnetic moment of Majorana neutrinos.

A stronger limit for the neutrino magnetic moment can be derived from well-known arguments against excessive cooling of red giant stars. A finite neutrino magnetic moment would enhance the plasmon decay into $\nu\overline{\nu}$ pairs in the stellar interior, resulting in excessive cooling. The most severe constraint is derived by estimating the critical mass for a helium flash in red giant stars. This gives the bound [18]

$$\mu_\nu < 3 \times 10^{-12} \mu_B \tag{3}$$

for the transition magnetic moment of Majorana neutrinos.

A magnetic moment of order $(10^{-12} - 10^{-10})\mu_B$ is very large in the context of the small neutrino masses we might consider here. In general, this is because the diagram that generates a magnetic moment of order $10^{-12}\mu_B$ or larger with the photon line removed also induces a large neutrino mass. There are many (successful but not compelling) attempts at constructing a mechanism to induce a large neutrino magnetic moment, while keeping the masses of neutrinos small [19]. Since these issues are very speculative, we will assume here that a neutrino transition magnetic moment of order $10^{-12}\mu_B$ is plausible. However, we will see that the crucial quantity governing the effects of RSFP in supernovae is the product of the neutrino transition magnetic moment and the magnetic field.

II. RESONANT NEUTRINO SPIN-FLAVOR PRECESSION IN SUPERNOVAE

In this section we discuss some general features of RSFP in supernovae. We also examine the case where *both* matter-enhanced MSW flavor conversion *and* RSFP occur in the region above the hot protoneutron star. Both Dirac and Majorana neutrinos can have RSFP, so long as the transition magnetic moment exists. The mechanism of RSFP is essentially the same for both cases. However, the implications of

RSFP for supernova heavy element nucleosynthesis and/or explosion dynamics will be very different for the two cases. This is because RSFP for Majorana neutrinos occurs between two active neutrinos, whereas RSFP for Dirac neutrinos occurs between active and sterile neutrino states. In this paper we shall consider only the Majorana neutrino case.

The Lagrangian which describes the magnetic moment-mediated interaction between Majorana neutrinos and the electromagnetic field $F_{\alpha\beta}$ is given by

$$\mathcal{L}_{\mathrm{int}} = \tfrac{1}{2}(\mu)_{ab}(\bar{\nu}_L)_a^C \sigma_{\alpha\beta}(\nu_L)_b F^{\alpha\beta} + \mathrm{H.c.}, \tag{4}$$

where $(\mu)_{ab}$ is the magnetic moment matrix with a, $b = e$, μ, τ, or 1, 2, 3 for the flavor or mass eigenstate bases, $\sigma_{\alpha\beta} = (i/2)[\gamma_\alpha, \gamma_\beta]$ with γ_α the Dirac matrices, and C denotes the operation of charge conjugation. From the requirement for CPT invariance, the diagonal elements of the magnetic moment μ_{aa} vanish, and consequently a transition magnetic moment is the only possibility for Majorana neutrinos. In the case of a finite neutrino transition magnetic moment, the presence of magnetic fields can facilitate the transformation $\nu_{aL} \to (\nu_{bL})^C$ ($a \neq b$) or vice versa. Since $(\nu_{bL})^C$ is generally termed $\bar{\nu}_b$ (antineutrino state for ν_b) and is right handed, we can describe the $\nu_a \leftrightarrow \bar{\nu}_b$ ($a \neq b$) transformation as a ''spin-flavor'' precession (or conversion). Except for the interaction in Eq. (4), we will assume here that neutrinos possess only standard electroweak interactions with matter.

Among the several conceivable channels of spin-flavorprecession, $\nu_{\tau(\mu)} \leftrightarrow \bar{\nu}_e$ is the example we will consider in what follows. Motivated by the average neutrino energy hierarchy discussed in the last section, we anticipate that this channel of RSFP may give the most significant effect on the electron fraction. We will show that the spin-flavor conversion of ν_τ (or ν_μ) with masses in the range 1–100 eV into a light $\bar{\nu}_e$ can result in important effects on the parameters which determine heavy element nucleosynthesis and/or shock reheating in the region above the neutrinosphere in supernovae. Hereafter, we will assume in this paper that ν_τ is the heavy neutrino with a mass in the range 1–100 eV, and we will consider the two generation system of electron and tau neutrinos only. Obviously, our computed effects in the supernova would be identical if instead we were to choose ν_μ as the heavy neutrino. This follows since we expect the energy spectra of ν_μ and ν_τ and their antiparticles to be nearly identical in our region of interest in supernovae. Working only with two neutrino generations is justified, so long as we assume that there exists a reasonable hierarchy of the three neutrino masses in which no degeneracy occurs.

The Majorana neutrino evolution equation for two neutrino generations, including a vacuum mixing angle, a transition magnetic moment, and magnetic fields, is given by [1]

$$i \frac{d}{dr} \begin{bmatrix} \nu_e \\ \nu_\tau \\ \bar{\nu}_e \\ \bar{\nu}_\tau \end{bmatrix} = H \begin{bmatrix} \nu_e \\ \nu_\tau \\ \bar{\nu}_e \\ \bar{\nu}_\tau \end{bmatrix}, \tag{5}$$

$$H = \begin{bmatrix} a_{\nu_e} + \Delta \sin^2\theta & \tfrac{1}{2}\Delta \sin 2\theta & 0 & \mu_\nu B_\perp \\ \tfrac{1}{2}\Delta \sin 2\theta & a_{\nu_\tau} + \Delta \cos^2\theta & -\mu_\nu B_\perp & 0 \\ 0 & -\mu_\nu B_\perp & -a_{\nu_e} + \Delta \sin^2\theta & \tfrac{1}{2}\Delta \sin 2\theta \\ \mu_\nu B_\perp & 0 & \tfrac{1}{2}\Delta \sin 2\theta & -a_{\nu_\tau} + \Delta \cos^2\theta \end{bmatrix}, \tag{6}$$

where θ is the vacuum mixing angle, and μ_ν is the transition magnetic moment between ν_e and $\bar{\nu}_\tau$. Here $B_\perp$ is the transverse component of the magnetic field along the neutrino trajectory. In the usual fashion we define $\Delta \equiv \delta m^2/2E_\nu$, where $\delta m^2 \equiv m_2^2 - m_1^2 > 0$ is the difference of the squared vacuum mass eigenvalues of the two neutrino mass eigenstates $\nu_2 \sim \nu_\tau$ and $\nu_1 \sim \nu_e$, and E_ν is the neutrino energy. We assume that the vacuum mixing angle θ is very small, so that in vacuum with no magnetic fields the mass eigenstates are approximately coincident with the flavor eigenstates. The effective matter potentials for ν_e and ν_τ are given by

$$a_{\nu_e} = \sqrt{2} G_F (n_e - \tfrac{1}{2} n_n), \tag{7}$$

$$a_{\nu_\tau} = \sqrt{2} G_F (-\tfrac{1}{2} n_n), \tag{8}$$

where G_F is the Fermi constant, n_e and n_n are the net number densities of electrons and neutrons, respectively. These expressions are for a neutral unpolarized medium and we neglect the contribution from neutrino-neutrino scattering because its effect would be small under the conditions we consider here (see Ref. [20] for detailed studies of neutrino-neutrino scattering effect on MSW neutrino flavor transformation). In Eq. (6), n_e, n_n, and $B_\perp$ are all understood to be position dependent in the region above the neutrinosphere which we consider here.

By equating each two of the diagonal elements in the Hamiltonian matrix in Eq. (6), we find that there are two kinds of resonances. As expected, these correspond to MSW conversion and RSFP. The MSW resonance occurs when

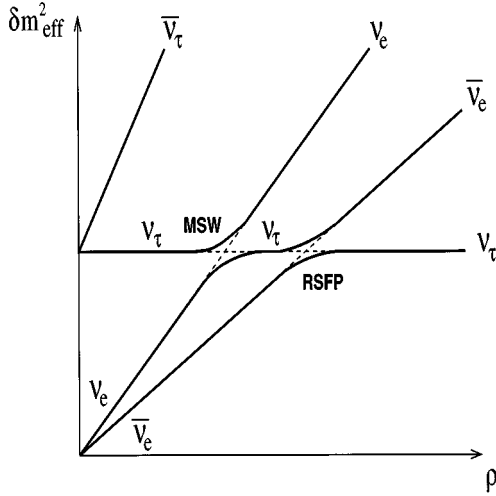$$\sqrt{2} G_F n_e = \Delta \cos 2\theta. \tag{9}$$

FIG. 1. Schematic picture of the RSFP and MSW resonances for two generations of Majorana neutrinos. Each curve shows the effective neutrino mass-squared difference as a function of the matter density in neutron-rich ($\frac{1}{3} < Y_e < \frac{1}{2}$) matter in the presence of a magnetic field, including effects of a neutrino vacuum mixing angle and a neutrino transition magnetic moment.

The RSFP resonance occurs when

$$\sqrt{2} G_F(n_e - n_n) = \pm \Delta \, \cos 2\theta, \qquad (10)$$

where the plus sign is for the ν_e-$\overline{\nu}_\tau$ resonance and the minus sign is for the $\overline{\nu}_e$-ν_τ resonance. These two RSFP resonances cannot occur at the same time. As can be readily seen from Eq. (10), the ν_e-$\overline{\nu}_\tau$ resonance occurs if the sign of $n_e - n_n$ is positive, whereas the $\overline{\nu}_e$-ν_τ resonance occurs if the sign of $n_e - n_n$ is negative at the resonance position.

The resonance region of most interest here lies above the neutrinosphere, but at an early epoch ($t_{PB} \approx 0.1$–0.6 s), within the radius where the shock has stalled ($r \approx 500$ km) and/or, at a later epoch ($t_{PB} \approx 3$–20 s), within the radius where the weak and/or nuclear reactions freeze out ($r \approx 40$ km). Here, t_{PB} indicates the time *post core bounce*. In the standard supernova models, $n_e - n_n$ takes negative values in the regions of interest. Hence, the relevant RSFP we will consider is $\overline{\nu}_e \leftrightarrow \nu_\tau$. For a neutral medium ($n_e = n_p$), the neutron excess can be characterized by the electron fraction Y_e, the net number of electrons per baryon:

$$Y_e \equiv \frac{n_e}{n_e + n_n}. \qquad (11)$$

If $Y_e < 0.5$ then $n_n > n_e$. From numerical supernova models, the typical values of Y_e are predicted to be about 0.4–0.45 in the region of interest above the neutrinosphere [21].

In Fig. 1 we have plotted schematically as functions of matter density ρ the neutrino energy levels (effective mass-squared differences) in neutron-rich environments ($n_n > n_p$) for two generations of Majorana neutrinos. To draw the curves in this figure we have assumed that $\frac{1}{3} < Y_e < \frac{1}{2}$. This condition on the electron fraction should be valid so long as we confine our considerations to the region well above the neutrinosphere. The number density of electrons and neutrons are related to matter density ρ in the following manner:

$$n_e = \rho Y_e N_A, \qquad (12)$$

$$n_n = \rho(1 - Y_e) N_A, \qquad (13)$$

where N_A is Avogadro's number. The resonance density for RSFP is given by

$$\rho_{res}^{RSFP} \approx 6.6 \times 10^7 \left[\frac{\delta m^2}{100 \ eV^2}\right]\left[\frac{10 \ MeV}{E_\nu}\right] \frac{\cos 2\theta}{1 - 2Y_e} \ g \ cm^{-3}, \qquad (14)$$

whereas the MSW resonance density is

$$\rho_{res}^{MSW} = \frac{1 - 2Y_e}{Y_e} \rho_{res}^{RSFP}. \qquad (15)$$

As one can see from Eq. (15), the resonance density for RSFP is larger than that for MSW conversion as long as $\frac{1}{3} < Y_e < \frac{1}{2}$. This implies that the RSFP resonance takes place *before* the MSW resonance as neutrinos propagate from the neutrinosphere to the outer regions of the supernova (see Fig. 1). Since the matter density at the neutrinosphere is $\gtrsim 10^{12}$ g cm^{-3}, neutrinos with typical energies and possessing cosmologically significant masses (1–100 eV) will propagate through one or more resonances.

In order to illustrate the mechanism of RSFP, let us first work with the system of $\overline{\nu}_e$ and ν_τ alone, and ignore for the time being MSW flavor conversion. However, it should be noted that the following discussion of the effects of RSFP will be valid even if the MSW resonance were to coexist with RSFP, so long as the two resonances are well separated [see Eq. (27) for the nonoverlapping condition for the two resonances]. In the limit where the vacuum mixing angle is vanishingly small, $\theta \to 0$, Eq. (5) can be reduced to the expression

$$i \frac{d}{dr}\begin{bmatrix} \overline{\nu}_e \\ \nu_\tau \end{bmatrix} = \begin{bmatrix} -a_{\nu_e} & -\mu_\nu B \\ -\mu_\nu B & a_{\nu_\tau} + \Delta \end{bmatrix}\begin{bmatrix} \overline{\nu}_e \\ \nu_\tau \end{bmatrix}. \qquad (16)$$

In this equation and hereafter we will simply write B where we have written $B_\perp$ before. However, it should be understood always that only the transverse component of the magnetic field along neutrino trajectories is relevant for neutrino spin-flavor precession. The resonance condition for RSFP in this case is given by

$$\sqrt{2} G_F(n_n - n_e) = \Delta, \qquad (17)$$

where it is assumed that $n_n - n_e > 0$. At resonance, the transformation between $\overline{\nu}_e$ and ν_τ can be greatly enhanced even if $\mu_\nu B_{res} \ll \Delta$, since the matter potential cancels the mass difference between $\overline{\nu}_e$ and ν_τ at this position [see Eq. (17)]. Here B_{res} is the magnitude of the transverse magnetic field at resonance. At least in a mathematical sense, the RSFP level crossing is very similar to the MSW one.

The effective mixing angle $\widetilde{\theta}$ and the precession length L in the supernova environment are given by

$$\sin 2\widetilde{\theta} = \frac{2\mu_\nu B}{\{(2\mu_\nu B)^2 + [\Delta - \sqrt{2} G_F(n_n - n_e)]^2\}^{1/2}}, \qquad (18)$$

$$L = \frac{2\pi}{\{(2\mu_\nu B)^2 + [\Delta - \sqrt{2}G_F(n_n - n_e)]^2\}^{1/2}}. \qquad (19)$$

The precession length at the RSFP resonance is

$$L_{\text{res}} = \frac{\pi}{\mu_\nu B_{\text{res}}} \approx 1.1 \times 10^4 \ \text{cm} \left[\frac{\mu_B \ \text{G}}{\mu_\nu B_{\text{res}}}\right], \qquad (20)$$

where $\mu_B \equiv e/2m_e$ is the Bohr magneton. The width of the RSFP resonance is given by

$$\delta r = 2H \tan 2\widetilde{\theta}_0, \qquad (21)$$

where

$$\tan 2\widetilde{\theta}_0 \equiv 2\mu_\nu B_{\text{res}}/\Delta$$

$$\approx 2.3 \times 10^{-3} \left[\frac{\mu_\nu B_{\text{res}}}{\mu_B \ \text{G}}\right]\left[\frac{100 \ \text{eV}^2}{\delta m^2}\right]\left[\frac{E_\nu}{10 \ \text{MeV}}\right]. \qquad (22)$$

Here H is the ''density'' scale height which can be expressed as

$$H \equiv \left|\frac{d}{dr} \ln(n_n - n_e)\right|_{\text{res}}^{-1} \approx \left|\frac{d}{dr} \ln\rho\right|_{\text{res}}^{-1}. \qquad (23)$$

To derive Eq. (23) we have assumed that $|dY_e/dr|$ is very small compared with $|d \ln\rho/dr|$. This approximation is valid in the region above the neutrinosphere where RSFP can significantly affect supernova dynamics and/or nucleosynthesis.

Adiabatic spin-flavor conversion takes place when the condition $L_{\text{res}} \ll \delta r$ obtains. When $\tan 2\widetilde{\theta}_0 \ll 1$, we can employ the simple Landau-Zener approximation to estimate the probability for a ν_τ (or $\bar{\nu}_e$) going through the RSFP resonance to remain as a ν_τ (or $\bar{\nu}_e$). This probability is given by

$$P_{\text{RSFP}} \approx \exp\left(-\frac{\pi^2}{2}\frac{\delta r}{L_{\text{res}}}\right)$$

$$\approx \exp\left\{-0.2\left[\frac{\mu_\nu B_{\text{res}}}{\mu_B \ \text{G}}\right]^2\left[\frac{100 \ \text{eV}^2}{\delta m^2}\right]\left[\frac{E_\nu}{10 \ \text{MeV}}\right]\right.$$

$$\left. \times \left[\frac{H}{10^5 \ \text{cm}}\right]\right\}. \qquad (24)$$

It should be noted that the dependence of this probability on E_ν and δm^2 is opposite to the corresponding depence of the MSW survival probability [see Eq. (28)].

It is conceivable that we may encounter situations where perhaps the magnetic fields are very large, or neutrino transition magnetic moments are nearly at the maximum values allowed by experiment. Such a situation, in turn, could lead to large precession effects when $\tan 2\widetilde{\theta}_0 \sim 1$. To properly treat the RSFP survival probabilities in this case, we should employ the following more appropriate formula [22] instead of Eq. (24):

$$P_{\text{RSFP}} \approx \frac{1}{2} + \left[\frac{1}{2} - \exp\left(-\frac{\pi^2}{2}\frac{\delta r}{L_{\text{res}}}\right)\right]\cos 2\widetilde{\theta}_i \cos 2\widetilde{\theta}_f, \qquad (25)$$
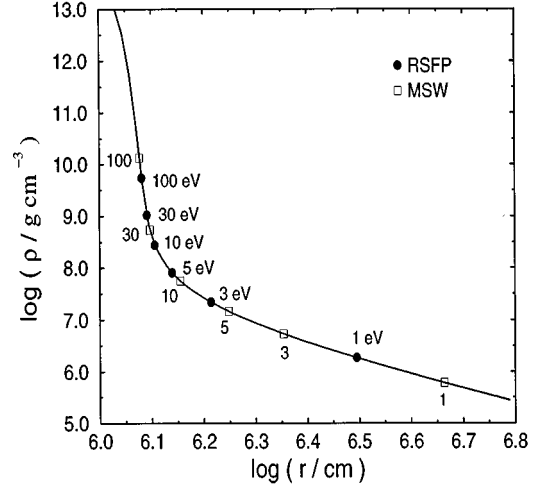
where

FIG. 2. A typical matter density profile from numerical supernova models at late times ($t_{\text{PB}} = 5.8$ s). Filled circles and open squares show the positions of RSFP and MSW resonances, respectively, for a neutrino with $E_\nu = 25$ MeV and for the cases where the heavier vacuum neutrino masses are 100, 30, 10, 5, 3, and 1 eV. Numbers with ''eV'' are for RSFP resonances, whereas numbers without ''eV'' are for MSW resonances. The logarithm is to base 10.

$$\cos 2\widetilde{\theta}_{i(f)} = \frac{\Delta - \sqrt{2}G_F(n_n - n_e)}{\{(2\mu_\nu B)^2 + [\Delta - \sqrt{2}G_F(n_n - n_e)]^2\}^{1/2}}\Bigg|_{r = r_{i(f)}}. \qquad (26)$$

Here, $\widetilde{\theta}_i$ is the initial mixing angle at radius r_i where neutrinos are produced (neutrinosphere), and $\widetilde{\theta}_f$ is the final mixing angle at radius r_f where we calculate the survival probabilities. The initial mixing angle at the neutrinosphere always satisfies $\cos 2\widetilde{\theta}_i \approx -1$ for $\mu_\nu B(r_i) \lesssim 10\mu_B$ G, whereas $\cos 2\widetilde{\theta}_f \approx 1$ unless $2\mu_\nu B(r_f) \gtrsim \Delta$. For our choice of parameters in Secs. III and IV, Eqs. (24) and (25) give almost identical probabilities except around $\delta m^2 \sim 1$ eV^2.

Let us now consider the case where both MSW and RSFP resonances occur along a neutrino trajectory. As one can see from Eq. (15), the resonance densities for MSW conversion and RSFP will necessarily be different for $Y_e \neq \frac{1}{3}$. This in turn implies that the MSW and RSFP resonances will occur at different distances from the neutron star. In Fig. 2 we plot a typical matter density profile at late times, which corresponds to $t_{\text{PB}} \approx 6$ s in a numerical supernova model by Wilson and Mayle [21]. In this figure we also indicate the resonance positions for RSFP (filled circles) and MSW conversion (open squares) for a neutrino with $E_\nu = 25$ MeV and for various labeled heavier vacuum neutrino mass eigenvalues. In labeling these resonance positions we have assumed that $\delta m^2 = m_2^2 - m_1^2 \approx m_2^2$. Note that the matter density at the neutrinosphere is about 10^{12} g cm^{-3}. In Fig. 3 we plot the resonance positions (log of the radius in cm) for MSW conversion (dashed line) and RSFP (solid line) as functions of δm^2. From Figs. 2 and 3, we can clearly see that for a given neutrino energy, the RSFP resonance occurs at higher density than the MSW resonance, unless $\delta m^2 > 1000$ eV^2.
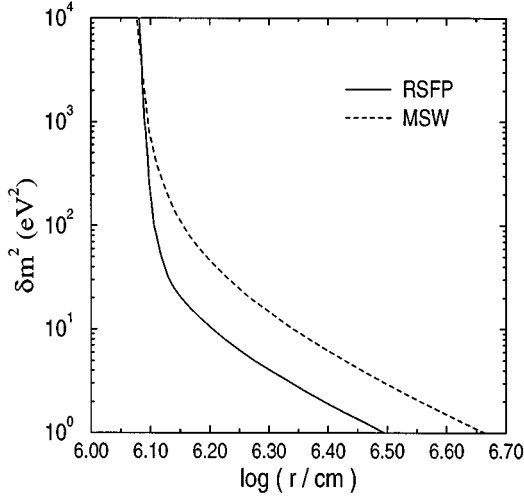
FIG. 3. Positions for RSFP (solid line) and MSW (dashed line) resonances for different values of δm^2. These resonance positions are for a neutrino with $E_\nu = 25$ MeV and correspond to the matter density profile in Fig. 2. The logarithm is to base 10.

An analytic treatment of the case where both RSFP and MSW resonances occur along a neutrino path is possible if the two resonances are well separated in space. The nonoverlapping condition for these two resonances is given by [23]

$$(3Y_e - 1)/Y_e > \tan 2\theta + \tan 2\widetilde{\theta}_0. \tag{27}$$

If this condition is not satisfied, we would have to do a numerical integration of Eq. (5) to estimate reliably the survival probabilities. The above inequality holds for almost all of the parameter region we will discuss in Secs. III and IV. The probability for a ν_e (or ν_τ) going through the MSW resonance to remain as a ν_e (or ν_τ) is given by

$$
\begin{aligned}
P_{\text{MSW}} &\approx \exp\!\left(-\frac{\pi}{2} H\Delta \sin^2 2\theta \right) \\
&\approx \exp\!\left\{ -0.4 \left[\frac{\delta m^2}{100 \text{ eV}^2} \right]\!\left[\frac{10 \text{ MeV}}{E_\nu} \right]\!\left[\frac{H}{10^5 \text{ cm}} \right] \right. \\
&\qquad\left. \times \left[\frac{\sin^2 2\theta}{10^{-5}} \right] \right\},
\end{aligned}
\tag{28}
$$

for $\theta \ll 1$. In Eq. (28), we have made the approximation $|d \ln n_e/dr|^{-1} \approx |d \ln\rho/dr|^{-1} \approx H$. In Fig. 4 we plot the more accurate ''density'' scale heights for the RSFP (solid line) and MSW (dashed line) resonances as functions of $n_n - n_e$ and n_e, respectively.

By employing Eqs. (25) and (28), we can easily estimate the probability that a ν_τ emitted from the neutrinosphere, and subsequently propagating through an RSFP resonance and then later through an MSW resonance, emerges as ν_τ, ν_e, or $\overline{\nu}_e$ to be

$$P(\nu_\tau \to \nu_\tau) = P_{\text{RSFP}} P_{\text{MSW}}, \tag{29}$$

$$P(\nu_\tau \to \nu_e) = P_{\text{RSFP}}[1 - P_{\text{MSW}}], \tag{30}$$

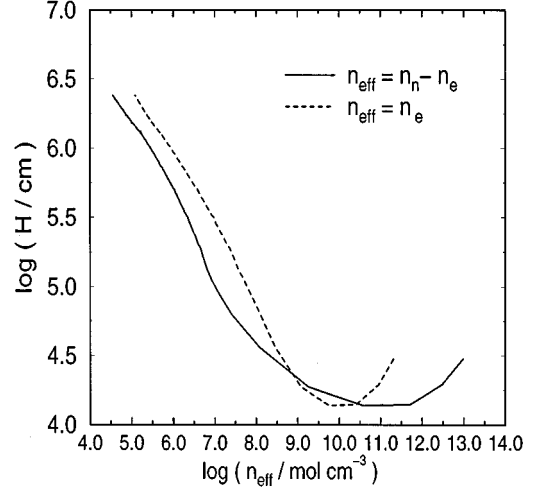$$P(\nu_\tau \to \overline{\nu}_e) = 1 - P_{\text{RSFP}}. \tag{31}$$

FIG. 4. ''Density'' scale heights H as functions of $n_n - n_e$ (RSFP) and n_e (MSW) corresponding to the matter density profile in Fig. 2. The logarithm is to base 10.

Other probabilities such as $P(\overline{\nu}_e \to \nu_\tau)$ and $P(\nu_e \to \nu_\tau)$ can be estimated in a straightforward and similar fashion.

III. NEUTRINO SPIN-FLAVOR CONVERSION AND HOT BUBBLE r-PROCESS NUCLEOSYNTHESIS

In the post-core-bounce evolution of the hot protoneutron star, all six species of neutrinos and antineutrinos are produced thermally, provided that all vacuum neutrino masses are reasonably light. These neutrinos carry away the gravitational binding energy of the neutron star on a neutrino diffusion time scale. This time scale is roughly ~ 10 s and is essentially set by three quantities: the mass of the neutron star (roughly the Chandrasekhar mass), the saturation density of nuclear matter, and the Fermi constant G_F. The neutrino diffusion process sets the time scale for all of the post-core-bounce supernova evolution. We have explained in the introduction that we expect the neutrinos emitted from the neutrinosphere to be instrumental in heating and ejecting the envelope of material which surrounds the neutron star. For our purposes it is convenient, if somewhat artificial, to divide the evolution of this envelope into two epochs: the epoch of shock reheating at $t_{\text{PB}} < 1$ s, and the hot bubble r-process epoch at $t_{\text{PB}} \approx 3$–20 s. In addition to the neutrino diffusion time scale, the neutron star radius, the weak and nuclear freeze-out positions, and the location of the rapid neutron capture environment, there is yet one more important characteristic length scale in the hot bubble or wind environment—the gain radius. Heating engendered by charged-current absorption of electron neutrinos and antineutrinos on nucleons wins out over neutrino losses in the hot plasma above the ''gain radius,'' $r_g \gtrsim 10$ km [11,24].

As outlined in Sec. I, early deleptonization of the hot protoneutron star causes its outer layers to become neutron rich. This neutron excess causes ν_e to have a larger opacity than $\overline{\nu}_e$ because of the charged-current capture reactions on free nucleons in Eqs. (1a) and (1b). Consequently, $\overline{\nu}_e$ have a larger average energy than ν_e because $\overline{\nu}_e$ decouple deeper in the core where the matter is hotter. The typical average energies for ν_e and $\overline{\nu}_e$ at the hot bubble r-process epoch are 11

and 16 MeV, respectively. On the other hand, the typical average energies of ν_μ, $\overline{\nu}_\mu$, ν_τ, and $\overline{\nu}_\tau$ are all about 25 MeV. This is because they only have the neutral-current reaction opacity sources common to all neutrino species. Hence, ν_μ, $\overline{\nu}_\mu$, ν_τ, and $\overline{\nu}_\tau$ decouple in regions hotter than those where ν_e and $\overline{\nu}_e$ decouple. Thus, the average neutrino energies in supernovae during the post-core-bounce epoch always satisfy the hierarchy

$$\langle E_{\nu_{\tau(\mu)}} \rangle \approx \langle E_{\overline{\nu}_{\tau(\mu)}} \rangle > \langle E_{\overline{\nu}_e} \rangle > \langle E_{\nu_e} \rangle. \qquad (32)$$

The value of Y_e in the region above the neutrinosphere is determined by the charged-current reactions in Eqs. (1a) and (1b). The rate of change of Y_e with time t or radius r in this region is given by

$$\frac{dY_e}{dt} = v(r)\frac{dY_e}{dr} = \lambda_1 - \lambda_2 Y_e, \qquad (33)$$

where $v(r)$ is the radial velocity field of the material in the supernova. In this equation, $\lambda_1 = \lambda_{\nu_e n} + \lambda_{e^+ n}$ and $\lambda_2 = \lambda_1 + \lambda_{\overline{\nu}_e p} + \lambda_{e^- p}$. Here, $\lambda_{\nu_e n}$ and $\lambda_{\overline{\nu}_e p}$ denote the rates for the reactions in Eqs. (1a) and (1b), respectively, and $\lambda_{e^- p}$ and $\lambda_{e^+ n}$ denote the rates for their reverse reactions. At some point above the neutrinosphere the local material expansion rate in the hot bubble will be faster than the rates of the reactions in Eqs. (1a) and (1b). We shall term this location the weak freeze-out point, since the value of Y_e for the material flow above this point will remain constant in time and space. Above the weak freeze-out point the solution of Eq. (33) gives

$$Y_e(r_{\rm NFO}) \approx Y_e(r_{\rm WFO}) \approx \frac{1}{1 + \lambda_{\overline{\nu}_e p}(r_{\rm WFO})/\lambda_{\nu_e n}(r_{\rm WFO})}, \qquad (34)$$

where $r_{\rm NFO}$ and $r_{\rm WFO}$ are the nuclear and weak freeze-out radius, respectively. Here we have neglected $\lambda_{e^- p}$ and $\lambda_{e^+ n}$. This is a valid approximation for our purposes, since the matter temperature in the region above the gain radius is small compared with the effective temperatures for ν_e and $\overline{\nu}_e$ energy distributions, and hence they are small compared with $\lambda_{\overline{\nu}_e p}$ and $\lambda_{\nu_e n}$.

The rate $\lambda_{\nu N}$ can be calculated as

$$\lambda_{\nu N} \approx \frac{L_\nu}{4\pi r^2} \frac{\int_0^\infty \sigma_{\nu N}(E_\nu) f_\nu(E_\nu) dE_\nu}{\int_0^\infty E_\nu f_\nu(E_\nu) dE_\nu}, \qquad (35)$$

with $(\nu, N) = (\nu_e, n)$ or $(\overline{\nu}_e, p)$. Here, L_ν is the neutrino luminosity, $f_\nu(E_\nu)$ is the normalized neutrino energy distribution function. We take $f_\nu(E_\nu)$ to be Fermi-Dirac with zero chemical potential in character for all neutrino species: i.e.,

$$f_\nu(E_\nu) = \frac{1}{1.803} \frac{1}{T_\nu^3} \frac{E_\nu^2}{1 + \exp[E_\nu/T_\nu]}, \qquad (36)$$

where T_ν is the neutrino temperature. The temperatures characterizing the distribution functions of each neutrino species at late epochs are approximately given by $T_{\nu_e} \approx 3.5$ MeV, $T_{\overline{\nu}_e} \approx 5.1$ MeV, and $T_{\nu_{\tau(\mu)}} \approx T_{\overline{\nu}_{\tau(\mu)}} \approx 7.9$ MeV. In Eq. (35),

$\sigma_{\nu N}$ is the cross section for the reactions in Eqs. (1a) and (1b), and is approximately given by

$$\sigma_{\nu N} \approx 9.6 \times 10^{-44} \left(\frac{E_\nu}{\rm MeV}\right)^2 {\rm cm}^2. \qquad (37)$$

Utilizing Eqs. (35)–(37), and taking into account that each neutrino species has roughly the same luminosity at late epochs, we can approximate Eq. (34) as

$$Y_e(r_{\rm NFO}) \approx \frac{1}{1 + \langle E_{\overline{\nu}_e} \rangle/\langle E_{\nu_e} \rangle} \approx \frac{1}{1 + T_{\overline{\nu}_e}/T_{\nu_e}}. \qquad (38)$$

For typical neutrino average energies $\langle E_{\overline{\nu}_e} \rangle = 16$ MeV and $\langle E_{\nu_e} \rangle = 11$ MeV, we obtain $Y_e \approx 0.41$. This value can be regarded as the standard supernova model prediction for the Y_e in the hot bubble in the absence of RSFP and MSW conversion.

Let us examine now how the value of Y_e would be affected by RSFP and MSW resonances occurring along neutrino trajectories below the weak freeze-out radius in the hot bubble. For this case, the computation of Y_e must employ the ''distorted'' energy distribution functions for $\overline{\nu}_e$ and ν_e which will result from the energy-dependent flavor conversion associated with the neutrino propagating through an RSFP and/or an MSW resonance. By using the survival probabilities calculated in Eqs. (24) and (28) in Sec. II at these RSFP and MSW resonances, we can estimate the effective $\overline{\nu}_e$ and ν_e energy distribution functions at the weak freeze-out radius to be

$$f_{\overline{\nu}_e}(E_\nu) = f_{\overline{\nu}_e}^0(E_\nu) P_{\rm RSFP}(E_\nu) + f_{\nu_\tau}^0(E_\nu)[1 - P_{\rm RSFP}(E_\nu)], \qquad (39)$$

$$\begin{aligned} f_{\nu_e}(E_\nu) = &f_{\nu_e}^0(E_\nu) P_{\rm MSW}(E_\nu) \\ &+ f_{\nu_e}^0(E_\nu)[1 - P_{\rm RSFP}(E_\nu)][1 - P_{\rm MSW}(E_\nu)] \\ &+ f_{\nu_\tau}^0(E_\nu) P_{\rm RSFP}(E_\nu)[1 - P_{\rm MSW}(E_\nu)]. \qquad (40) \end{aligned}$$

Here $f_\nu^0(E_\nu)$ represents the appropriate initial neutrino energy distribution function. As in Eq. (36), these initial neutrino energy distribution functions are all assumed to be Fermi-Dirac with zero chemical potential in character, but with different temperatures T_{ν_e}, $T_{\overline{\nu}_e}$, and T_{ν_τ}. By employing the distorted energy distribution functions for $\overline{\nu}_e$ and ν_e in Eqs. (39) and (40), respectively, we can use Eq. (35) to calculate the rate $\lambda_{\nu N}$, and hence Eq. (34) to estimate Y_e.

We can now describe the results of our calculation of Y_e for two cases: (1) RSFP but no MSW conversion along a neutrino trajectory, and (2) both RSFP and MSW conversion on the same neutrino path. In our calculations we assume that the magnetic field profiles around the protoneutron star are as follows:

$$B(r) = B_0(r_0/r)^n \times 10^{12} \ {\rm G}, \qquad (41)$$

where $r_0 = 10$ km and $n = 2$ or 3. A magnetic field of order 10^{12} G around the protoneutron star is plausible, especially given that some pulsar magnetic fields are at least this large. However, this argument should be viewed with some skepticism. There is no guarantee, for example, that the large pulsar magnetic fields are not generated only after the epoch of neutrino heating that we are investigating. Nevertheless,
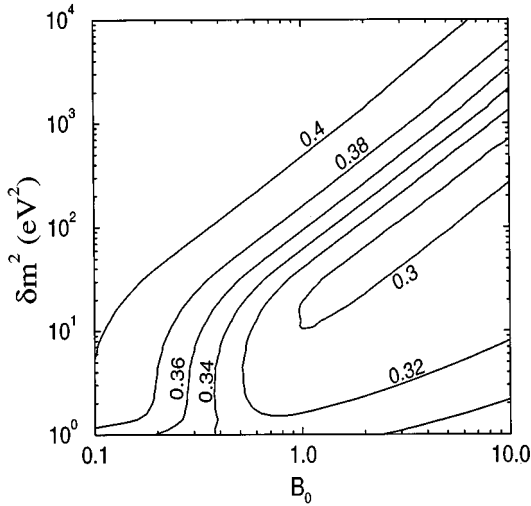
FIG. 5. Contour plot of Y_e in the B_0-δm^2 plane for the RSFP case where $B(r) = B_0(r_0/r)^2 \times 10^{12}$ G ($r_0 = 10$ km).

the RSFP effects which we describe actually depend on the product of the neutrino transition magnetic moment and the magnetic field component transverse to the neutrino trajectory. So in addition to any uncertainties in the magnetic field magnitude, there are geometric uncertainties due to the unknown distribution and orientation of the magnetic field, as well as the inherent uncertainties in the neutrino transition magnetic moment. For the purposes of our parametric study, we fix the value of the neutrino transition magnetic moment to be $\mu_\nu = 10^{-12} \mu_B$. Again, however, it should be noted that our results depend only on the combination of $\mu_\nu B_0$ for fixed value of n.

Let us first discuss case (1) where there is only RSFP and no MSW conversion. This case will obtain whenever $\sin^2 2\theta \lesssim 10^{-5}$ and $\delta m^2 \approx 1 - 10^4$ eV^2. We use the energy distributions in Eqs. (39) and (40) with $P_{\rm MSW} = 1$ to calculate the values of Y_e in this case. The initial and final mixing angles for RSFP in this case are taken to be at the neutrinosphere ($r \approx 10$ km) and the weak freeze-out radius ($r \approx 40$ km), respectively. In Fig. 5 we have plotted the contours of Y_e (as labeled) in the B_0-δm^2 plane for $B \propto r^{-2}$ ($n = 2$). These contours correspond to Y_e values at the weak freeze-out radius, above which r-process nucleosynthesis may be occurring. One can see from this figure that the value of Y_e is modified significantly from the standard no-RSFP case whenever $B_0 \gtrsim 0.1$. In Fig. 6 we have plotted the same contours as in Fig. 7, but for $B \propto r^{-3}$ ($n = 3$). Because of the rapid decrease of magnetic field for $n = 3$, the magnitude of B_0 required to cause similar effects on Y_e is somewhat larger than that for $n = 2$.

Next we examine case (2), where there exist both RSFP and MSW conversion along neutrino trajectories. In Fig. 7 we plot the regions in the $\sin^2 2\theta$-δm^2 parameter space where neutrino flavor evolution is dominated by RSFP and/or MSW conversion, or neither, for the matter density profile in Fig. 2. The solid and dashed lines correspond to $P_{\rm RSFP} = e^{-1}$ and $P_{\rm MSW} = e^{-1}$, respectively, for a neutrino with $E_\nu = 25$ MeV. We have taken $\mu_\nu B_{\rm res} = 1\mu_B$ G in drawing the solid line in Fig. 7. This figure clearly separates the parameter space into four regions, (a)–(d). In region (a), MSW conversion is nearly completely adiabatic and therefore very
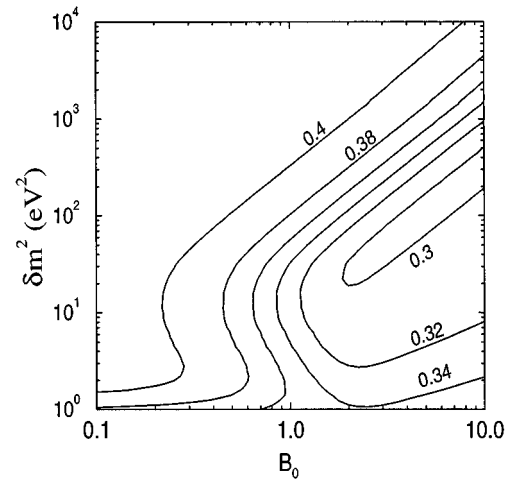
efficient in $\nu_e \leftrightarrow \nu_\tau$ conversion; whereas in region (b), RSFP is nearly completely adiabatic and thus quite efficient in $\bar{\nu}_e \leftrightarrow \nu_\tau$ conversion. In region (c), neutrino propagation is quite adiabatic through both the RSFP and MSW resonances; whereas in region (d), neutrino propagation through either type of resonance is nonadiabatic. The solid line in this figure would move upward to $\delta m^2 \approx 1000$ eV^2 if we were to take $\mu_\nu B_{\rm res} = 10\mu_B$ G, and downward to $\delta m^2 \approx 3$ eV^2 if we were to take $\mu_\nu B_{\rm res} = 0.1\mu_B$ G.

In the calculations for case (2), the initial mixing angle (required for estimating survival probabilities after neutrino propagation through an RSFP resonance) is evaluated at the neutrinosphere. This choice is not crucial to our results—it is only necessary that we evaluate the initial mixing angle in a region where the density is significantly larger than that at the resonance position. The final mixing angle $\widetilde{\theta}_f$ is also
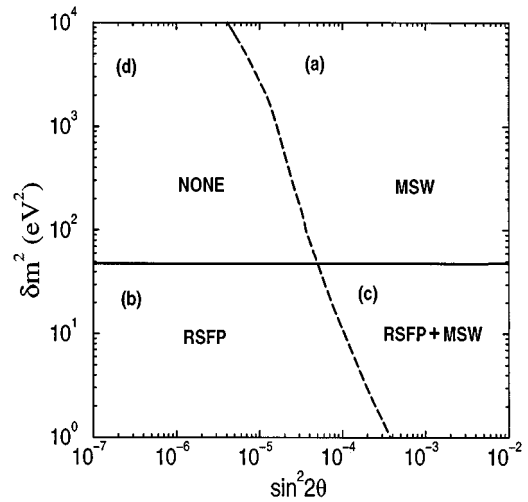

FIG. 7. Regions of the $\sin^2 2\theta$-δm^2 parameter space where neutrino flavor evolution is dominated by RSFP and/or MSW conversion, or neither, for the matter density profile in Fig. 2. The solid and dashed lines correspond to $P_{\rm RSFP} = e^{-1}$ and $P_{\rm MSW} = e^{-1}$, respectively, for a neutrino with $E_\nu = 25$ MeV. We take $\mu_\nu B_{\rm res} = 1\mu_B$ G in computing the location of the solid line.
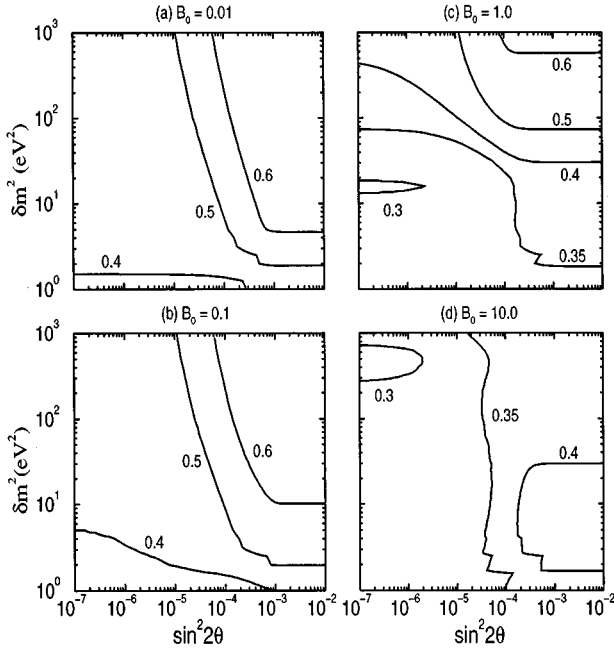

FIG. 6. Same as Fig. 5 but for the case where $B(r) = B_0(r_0/r)^3 \times 10^{12}$ G.

FIG. 8. Contour plots of Y_e in the $\sin^2 2\theta$-δm^2 plane for the cases where $B(r) = B_0(r_0/r)^2 \times 10^{12}$ G ($r_0 = 10$ km) with $B_0 = $ (a) 0.01, (b) 0.1, (c) 1.0, and (d) 10.0.

FIG. 9. Same as Fig. 8 but for the cases where $B(r) = B_0(r_0/r)^3 \times 10^{12}$ G with $B_0 = $ (a) 0.1, (b) 0.5, (c) 1.0, and (d) 10.0.

required for estimating RSFP survival probabilities. This angle must be evaluated at a radius lying somewhere above the RSFP resonance, but below the MSW resonance. We have used the following approximation to estimate $\widetilde{\theta}_f$:

$$\cos 2\widetilde{\theta}_f = \begin{cases} \cos 2\widetilde{\theta}|_{r=r_{\mathrm{MSW}}} & \text{if } r_{\mathrm{MSW}} < r_{\mathrm{WFO}}, \\ \cos 2\widetilde{\theta}|_{r=r_{\mathrm{WFO}}} & \text{if } r_{\mathrm{MSW}} > r_{\mathrm{WFO}}, \end{cases} \quad (42)$$

where r_{MSW} is the radius for the MSW resonance. The non-overlapping condition for the RSFP and MSW resonances in Eq. (27) described in Sec. II must be satisfied if we are to employ the analytic Landau-Zener formula for survival probabilities. Since the two resonances are well separated so long as $\delta m^2 \lesssim 1000$ eV^2, we choose to perform calculations for this parameter range only.

In Fig. 8 we have plotted contours of Y_e (as labeled) in the $\sin^2 2\theta$-δm^2 plane for the magnetic field profile of the form given in Eq. (41) with $n = 2$ and $B_0 = $ (a) 0.01, (b) 0.1, (c) 1.0, and (d) 10.0 on separate plots. In plots (a) and (b), the magnetic field is too small to cause appreciable RSFP, and thus we have obtained essentially the same results as in Ref. [9]. However, in plots (c) and (d), the contours corresponding to $Y_e = 0.5$ are significantly altered over the case without RSFP. In particular, in plot (d), where $B_0 = 10.0$, there is *no* parameter region where $Y_e > 0.5$. We have also done a similar set of calculations but now with $n = 3$ and $B_0 = $ (a) 0.1, (b) 0.5, (c) 1.0, and (d) 10.0. Contour plots for these calculations are given in Fig. 9. The overall qualitative behavior exhibited in Fig. 9 is similar to that in Fig. 8. From both Figs. 8 and 9 we can conclude that the effects of RSFP will dominate over those of MSW conversion alone whenever $B_0 \gtrsim 1.0$. Of course, this particular *quantitative* conclusion is predicated on neutrino transition magnetic moments being near their maximally allowed values. Obviously, smaller neutrino tran-
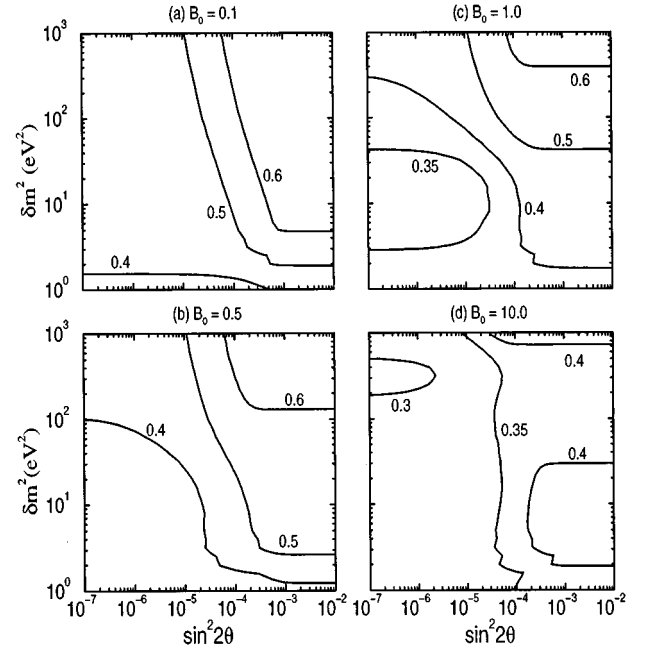
sition magnetic moments would then necessitate a larger threshold value of B_0 for which RSFP would dominate the effects on Y_e in the hot bubble.

IV. NEUTRINO SPIN-FLAVOR CONVERSION IN THE SHOCK REHEATING EPOCH

Neutrino propagation through RSFP resonances in the region above the neutrinosphere can also affect the dynamics of the supernova explosion. This comes about because flavor conversion in the region below the shock during the reheating epoch, $t_{\mathrm{PB}} \approx 0.1$–0.6 s, can lead to an enhanced neutrino energy deposition rate in this region which, in turn, can lead to a higher shock energy. For example, $\overline{\nu}_e$ in the reheating region would become more energetic if high energy ν_μ or ν_τ propagate through an RSFP resonance and become $\overline{\nu}_e$. This would lead to an enhanced $\overline{\nu}_e$ capture rate on protons, and hence an enhanced heating rate. Therefore, in what follows, we concentrate on how RSFP and/or MSW resonances influence the charged-current neutrino and antineutrino heating rates in the region below the shock.

The shock heating rate per proton or neutron is given by

$$\dot{\epsilon}_{\nu N} \approx \frac{L_\nu}{4\pi r^2} \frac{\int_0^\infty E_\nu f_\nu(E_\nu) \sigma_{\nu N} dE_\nu}{\int_0^\infty E_\nu f_\nu(E_\nu) dE_\nu}. \quad (43)$$

The total heating rate accompanying the ν_e and $\overline{\nu}_e$ absorption processes in Eqs. (1a) and (1b) is given by

$$\dot{\epsilon}_{\mathrm{tot}} = Y_n \dot{\epsilon}_{\nu_e n} + Y_p \dot{\epsilon}_{\overline{\nu}_e p}, \quad (44)$$

where Y_n and Y_p are the number fractions of free neutrons and protons, respectively, and are approximately specified by Eq. (34) as $Y_n \approx 1 - Y_e$ and $Y_p \approx Y_e$, respectively. The ratio of
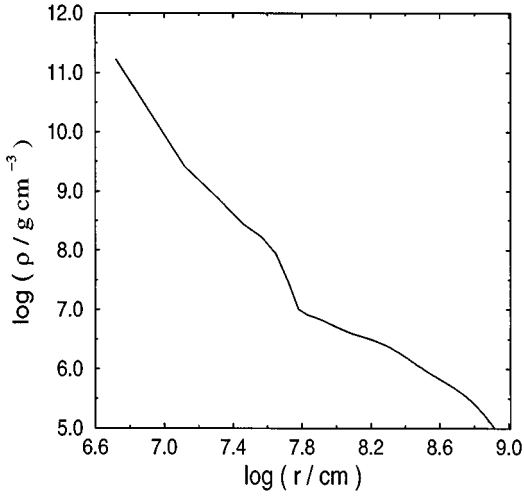
FIG. 10. A matter density profile from numerical supernova models at an early epoch ($t_{PB}=0.15$ s). The logarithm is to base 10.

the total heating rate with RSFP (primed symbols) to that without RSFP (and without MSW conversion) is given by

$$\frac{\dot{\epsilon}'_{tot}}{\dot{\epsilon}_{tot}} \approx \frac{Y'_n \dot{\epsilon}'_{\nu_e n} + Y'_p \dot{\epsilon}'_{\bar{\nu}_e p}}{Y_n \dot{\epsilon}_{\nu_e n} + Y_p \dot{\epsilon}_{\bar{\nu}_e p}}. \tag{45}$$

At a representative time during the reheating epoch, the temperatures of the relevant neutrino species are approximately given by $T_{\nu_{\tau(\mu)}} = T_{\bar{\nu}_{\tau(\mu)}} \approx 7$ MeV and $T_{\nu_e} \approx T_{\bar{\nu}_e} \approx 5$ MeV in the Wilson and Mayle calculations [21]. Thus, the ratio of the total heating rates with and without RSFP effects can be estimated to be

$$\frac{\dot{\epsilon}'_{tot}}{\dot{\epsilon}_{tot}} \approx Y'_n \left[1 + \frac{Y'_p}{Y'_n} \left(\frac{T_{\nu_\tau}}{T_{\nu_e}} \right)^2 \right] \approx \frac{T_{\nu_\tau}}{T_{\nu_e}} \approx 1.4, \tag{46}$$

where again we have taken the individual neutrino luminosities to be approximately the same. This estimate of the heating enhancement factor for RSFP has assumed complete $\nu_\tau \leftrightarrow \bar{\nu}_e$ conversion in the region below the shock. Because ν_e and $\bar{\nu}_e$ have roughly the same energy distributions at the reheating epoch, the heating enhancement factor and the accompanying Y_e value would remain essentially unchanged if additional MSW $\nu_\tau \leftrightarrow \nu_e$ conversion were to follow the complete $\nu_\tau \leftrightarrow \bar{\nu}_e$ conversion by RSFP. We should note that the absolute average energies and therefore the temperatures of the various neutrino species are a subject of great debate and controversy in the numerical supernova modeling community. However, it is clear that only the *differences* between the temperatures of the relevant neutrino species are important in our estimates of the reheating enhancement. Neutrino transport calculation estimates of these differences are somewhat more reliable than those of the average neutrino energies themselves.

In Fig. 10 we plot an example matter density profile in the region above the neutron star at an early epoch, $t_{PB}=0.15$ s, when shock reheating has commenced [21]. At this time in the Wilson and Mayle model the shock wave is located at $r \approx 4.7 \times 10^7$ cm from the neutron star center. Here we em-
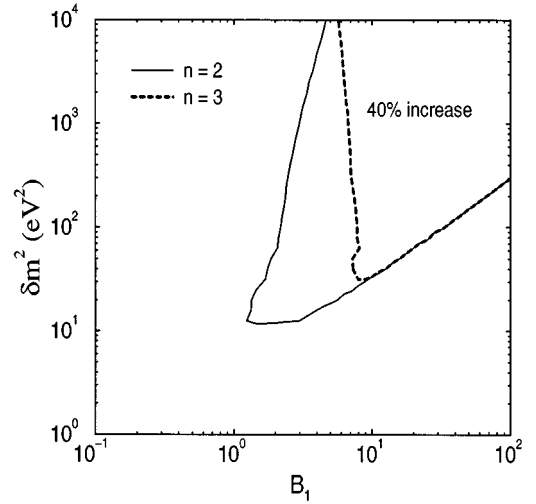

FIG. 11. Regions of the B_1-δm^2 parameter space where the increase in the total reheating rate is 40%. The solid and dashed lines are for the cases where $B(r)=B_1(r_1/r)^n \times 10^{12}$ G ($r_1=100$ km) with $n=2$ and 3, respectively.

ploy the same power-law-type magnetic field profiles as in Sec. III for our estimates of the shock reheating enhancement, i.e.,

$$B(r)=B_1(r_1/r)^n \times 10^{12} \text{ G}, \tag{47}$$

where $r_1=100$ km and $n=2$ or 3.

In Fig. 11 we plot the regions in the B_1-δm^2 parameter space where the enhancement of the reheating rate is 40%. Contours in this figure are shown for $n=2$ and 3, as represented by the solid and dashed lines, respectively, and are calculated from Eq. (45) with the use of Eqs. (34), (35), (39), and (43). If the parameters δm^2 and B_1 fall inside these contour lines, then the increase in the neutrino heating rate in the region below and near the shock is 40% more than that in the standard case without neutrino flavor mixing. We conclude that RSFP can produce heating effects which are similar to those discussed in Ref. [25] for the MSW conversion. Therefore, RSFP may be beneficial to models of the supernova explosion, by virtue of increasing the average $\bar{\nu}_e$ energy and leading to a more energetic shock wave. However, we should note that the larger neutron-to-proton ratio (lower Y_e) necessarily resulting from RSFP (as detailed in Sec. III) would aggravate the problem of overproduction of the $N=50$ nuclei, particularly, ^{88}Sr, ^{89}Y, and ^{90}Zr, which is inherent in some models of the nucleosynthesis from neutrino-heated supernova ejecta in this epoch [8].

V. CONCLUSIONS

We have investigated the combined effects of matter-enhanced MSW conversion and RSFP of Majorana neutrinos on supernova dynamics and heavy element nucleosynthesis in neutrino-heated supernova ejecta. If neutrinos are of Majorana-type and have transition magnetic moments of order $\sim 10^{-12}\mu_B$, then in the presence of a neutron star magnetic field of order $\sim 10^{12}$ G, resonant spin-flavor precession (conversion) of high energy ν_τ (or ν_μ) with vacuum masses in the range 1–100 eV into light $\bar{\nu}_e$ could increase the

neutron-to-seed ratio for the r process. In principle, RSFP could fix the central problem which confounds current models of r-process nucleosynthesis from late-time neutrino-heated supernova ejecta—obtaining a high enough neutron-to-seed ratio. We have found that significant enhancement in this ratio could be obtained for a plausible range of the protoneutron star magnetic field $B \gtrsim 10^{12}$ G and for neutrino transition magnetic moments near the maximum value allowed by the stringent astrophysical constraint. Although RSFP effects may enable r-process nucleosynthesis to proceed in the hot bubble, it does so at a price. The enhancement of the $\bar{\nu}_e$ energies resulting from RSFP may be at odds with the observations of these neutrinos from SN 1987A [13]. Of course, on the other hand, these considerations of the RSFP effects in supernovae may have important implications for cosmology, since the range of neutrino masses 1–100 eV required to obtain RSFP in the relevant region of the supernova is coincidently the range of interest for a significant neutrino dark matter component.

We have also shown here that r-process nucleosynthesis would not be suppressed even if the MSW resonance occurs along with the RSFP. This evasion of the bounds [9] from the r process on the MSW conversion will be operative so long as we can be guaranteed a large value of $\mu_\nu B_{\rm res} \gtrsim 1\mu_B$ G. For some of the parameters we considered, the value of Y_e can be as small as 0.3 when RSFP for high-energy neutrinos occurs near the weak freeze-out point. These very low values of Y_e are produced in our calculations when RSFP dominates neutrino flavor evolution. The existence of MSW resonances is irrelevant in this case.

We also examined the effects of RSFP during the shock reheating epoch. We found that RSFP can increase the total reheating rate by about 40%, but at the same time the concomitant reduction of Y_e would exacerbate the problem of the overproduction of the $N = 50$ nuclei at this epoch. This increase in total reheating rate *may be* welcome for the delayed supernova explosion mechanism, which relies on the energy deposited by ν_e and $\bar{\nu}_e$ absorption reactions above the neutrinosphere to power the shock. On the other hand, there is at present no compelling necessity in supernova models for an added boost in shock energy from a scheme such as the RSFP of supernova neutrinos. For example, Wilson and Mayle [21] obtained a supernova explosion energy in agreement with the SN 1987A observation by the delayed mechanism with ordinary neutrino heating alone.

[1] C. S. Lim and W. Marciano, Phys. Rev. D **37**, 1368 (1988).

[2] E. Akhmedov, Phys. Lett. B BAJ**213**, 64 (1988); See also, J. Schechter and J. W. F. Valle, Phys. Rev. D **24**, 1883 (1981); **25**, 283 (1982).

[3] S. P. Mikheyev and A. Yu. Smirnov, Sov. J. Nucl. Phys. **42**, 913 (1985); L. Wolfenstein, Phys. Rev. D **17**, 2369 (1978).

[4] E. Kh. Akhmedov, A. Lanza, S. T. Petcov, and D. W. Sciama, Phys. Rev. D **55**, 515 (1997).

[5] E. M. Burbidge, G. R. Burbidge, W. A. Fowler, and F. Hoyle, Rev. Mod. Phys. **29**, 547 (1957); A. G. W. Cameron, Publ. Astron. Soc. Pac. **69**, 201 (1957).

[6] S. E. Woosley and E. Baron, Astrophys. J. **391**, 228 (1992); S. E. Woosley, Astron. Astrophys. Suppl. Ser. **97**, 205 (1993).

[7] S. E. Woosley and R. D. Hoffman, Astrophys. J. **395**, 202 (1992); B. S. Meyer, G. J. Mathews, W. M. Howard, S. E. Woosley, and R. D. Hoffman, *ibid.* **399**, 656 (1992).

[8] S. E. Woosley, J. R. Wilson, G. J. Mathews, R. D. Hoffman, and B. S. Meyer, Astrophys. J. **433**, 229 (1994).

[9] Y.-Z. Qian, G. M. Fuller, G. J. Mathews, R. W. Mayle, J. R. Wilson, and S. E. Woosley, Phys. Rev. Lett. **71**, 1965 (1993).

[10] B. S. Meyer, Astrophys. J. **449**, L55 (1995).

[11] Y.-Z. Qian and S. E. Woosley, Astrophys. J. **471**, 331 (1996).

[12] R. D. Hoffman, S. E. Woosley, and Y.-Z. Qian, Astrophys. J. (to be published); B. S. Meyer, L. Luo, and B. Brown, report, 1996 (unpublished).

[13] G. M. Fuller, Y.-Z. Qian, and J. R. Wilson, in preparation.

[14] Y.-Z. Qian, Nucl. Phys. A (to be published).

[15] G. M. Fuller and B. S. Meyer, Astrophys. J. **453**, 792 (1995).

[16] R. D. Hoffman, S. E. Woosley, G. M. Fuller, and B. S. Meyer, Astrophys. J. **460**, 478 (1996).

[17] A. I. Derbin, A. V. Chernyi, L. A. Popeko, V. N. Muratova, G. A. Shishkina, and S. I. Bakhlanov, JETP Lett. **57**, 768 (1993).

[18] G. G. Raffelt, Phys. Rev. Lett. **64**, 2856 (1990).

[19] See for example, M. B. Voloshin, Sov. J. Nucl. Phys. **48**, 512 (1988); K. S. Babu and R. Mohapatra, Phys. Rev. Lett. **63**, 228 (1988); S. M. Barr, E. M. Freire, and A. Zee, *ibid.* **65**, 2626 (1990); D. Chang, W.-Y. Keung, S. Lipovaca, and G. Senjanovic, *ibid.* **67**, 953 (1991).

[20] Y.-Z. Qian and G. M. Fuller, Phys. Rev. D **51**, 1479 (1995); G. Sigl, Phys. Rev. D **51**, 4035 (1995).

[21] J. R. Wilson and R. W. Mayle (private communication).

[22] S. J. Parke and T. P. Walker, Phys. Rev. Lett. **57**, 2322 (1986); W. C. Haxton, Phys. Rev. D **36**, 2283 (1987).

[23] E. Kh. Akhmedov and Z. G. Berezhiani, Nucl. Phys. **B373**, 479 (1992).

[24] H. A. Bethe and J. R. Wilson, Astrophys. J. **263**, 386 (1985).

[25] G. M. Fuller, R. W. Mayle, B. S. Meyer, and J. R. Wilson, Astrophys. J. **389**, 517 (1992).